JOURNAL OF MATERIALS SCIENCE 32 (1997) 4183–4187

The influence of lateral stresses on brittle–ductile transitions in the die-compaction of sodium chloride

R. J. ROBERTS*, R. C. ROWE
ZENECA Pharmaceuticals, Alderley Park, Macclesfield, Cheshire SK10 2NA, UK
K. KENDALL
Keele University, Department of Chemistry, Keele, Staffordshire, ST5 5BG, UK

A model has been developed that accounts for the effect of lateral stresses on the deformation of particles occurring during die compaction. This has been examined using the model material sodium chloride. The lateral stresses were found to inhibit cracking of the particles during compaction. Agreement between the theory and experimental results was obtained.

1. Introduction

Both plastic and brittle deformation have been observed in sodium chloride particles during die compaction [1]. At a certain critical particle size there was a transition between plastic flow (for small particles) and cracking (for large particles). Reasonable agreement between theoretical predictions of the critical particle size, d_{crit} and experimental measurements determined from compaction of different size fractions at comparable strain rates was obtained [1]. The theory was based on critical stress intensity factors, K_{IC}, and indentation hardness, H, determined at comparable strain rates in separate measurements. However experimental deformation stresses determined from Heckel plots [2, 3] at large particle sizes (above 100 μm) were greater than theoretical predictions. This was attributed to simplifications in the theory and/or the influence of other particles in the powder bed. The purpose of this study is to explain this discrepancy by examining the influence of lateral stresses on crack growth which result from the interaction of other particles within the powder bed and die wall radial forces.

2. Theoretical considerations

For the axial splitting of a block of a brittle solid (Fig. 1) by a compressive load (X) with the application of a lateral compressive load (X_L) , it has been shown [4]

$$X = \left(\frac{2}{3}\right)^{1/2} \frac{d^{3/2} K_{IC}}{(1 - w/d)} + \frac{2X_L a}{(d - w)} \quad (1)$$

where w, d and a are shown in Fig. 1 and K_{IC} is the critical stress intensity factor. This relation shows that X_L causes a linear increase in X and that the increase is proportional to the crack length, a. Long cracks are therefore more inhibited than short cracks. Experiments [4] have confirmed the validity of this approach.

The purpose of this paper is to show that for die compaction, Equation 1 can be used to derive further equations which relate the deformation stress, σ_d, to the brittleness of the particles, accounting for the influence of lateral forces.

The lateral force, X_L, is a function of the radial stress component as a result of the interaction of other particles in the compacted powder bed. The radial stress, σ_r, will be a function of Poisson's ratio, porosity, contact area, interparticle and die-wall friction. For the purpose of the derivation, the lateral force, X_L, is taken as a function of the radial stress component, i.e.

$$X_L = \sigma_r C_A \quad (2)$$

where C_A is the contact area. Similarly for the axial force, X, a similar equation can be derived relating the contact area, C_A, and the axial stress or deformation stress, σ_d, in Equation 3

$$X = \sigma_d C_A \quad (3)$$

It is assumed that the contact area, C_A, is a function of the platten size, w, and the particle size, d, which presses onto the crack (Fig. 1) e.g. $C_A = wd$ as in Kendall's original derivation. Similarly the contact area for the lateral force is assumed to be of the same order. However the remaining problem is then to define the platten width in terms of the diameter of the particle, d. The change in failure mode from splitting to yielding takes place at a platten size of

* Author to whom correspondence should be addressed.

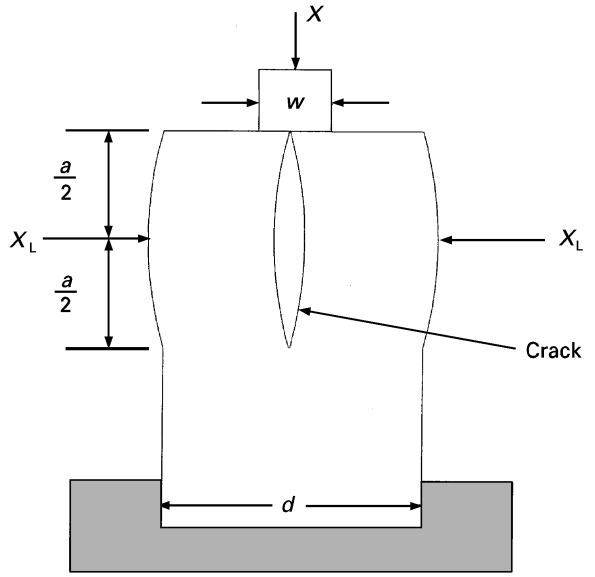

Figure 1 Compression geometry with a lateral force, X_L, which inhibit the bending of the struts.

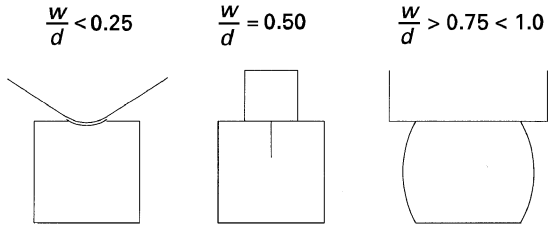

Figure 2 Various modes of crystal deformation during compressive loading.

$w/d = 1/2$ as shown by Kendall [4] and is represented by Equation 4

$$\frac{w}{d} = \frac{1}{2} \pm \left(\frac{1}{4} - \left(\frac{2K_{IC}^2}{3d\sigma_y^2}\right)^{1/2}\right)^{1/2} \quad (4)$$

where σ_y is the yield strength.

Kendall [4] showed that there were two wedge to particle size ratios, w/d, where there is a transition from fracture to plastic yielding. At the low w/d ratios [4] Kendall proposed that the wedge would act as an indenter and yielding would occur, although splitting might well occur due to the wedging action of the indenter. However, if a material was sufficiently soft or tough then splitting will never occur. At higher w/d ratios (at $w/d < 1$) yielding under the platten is also expected, since buckling of the struts is reduced because of radial movement from the action of the platten (i.e. frictional forces). The various modes are illustrated in Fig. 2, both these transitions are governed by Equation 4 [4]. Using this equation Kendall [4] explained the well known influence of platten geometry on compressive strength and the often reported variation in the compressive strength of materials could be rationalized based on changes in failure mode.

Using a ratio of $w/d = 1/2$ (where pure buckling of the struts occurs), $C_A = dw$ and since the radial stress is related to the deformation stress, i.e. $\sigma_r/\sigma_d = \Psi$ then Equations 2 and 3 become

$$X_L = \frac{\Psi\sigma_d d^2}{2} \quad (5)$$

and

$$X = \frac{\sigma_d d^2}{2} \quad (6)$$

Substituting these in Equation 1 gives

$$\frac{\sigma_d d^2}{2} = \left(\frac{2}{3}\right)^{1/2} \frac{d^{3/2}K_{IC}}{(1 - w/d)} + \frac{\Psi\sigma_d d^2 a}{(d - w)} \quad (7)$$

Using $w/d = 1/2$ and rearranging Equation 7

$$\sigma_d = \left(\frac{32}{3}\right)^{1/2} \frac{K_{IC}}{d^{1/2}} + \frac{4\Psi\sigma_d a}{d} \quad (8)$$

It should be noted that when the crack length a is zero, as at the brittle/ductile transition, e.g. $d = d_{crit}$, then the first term in Equation 8 is the same as that derived [5] (i.e. Equation 9, as used in previous work [1]).

$$\sigma_d = \left(\frac{32}{3}\right)^{1/2} \frac{K_{IC}}{d^{1/2}} \quad (9)$$

When the mode of deformation of the powder bed is dominated by brittle fracture then $\sigma_d = \sigma_f$ (fracture stress) and Equation 9 can be used to determine the fracture stress. Where plastic flow is the dominant deformation mechanism (e.g. below the brittle/ductile transition) then $\sigma_d = \sigma_y$ (yield stress).

Furthermore Equation 8 can be rearranged to give

$$\frac{a}{d} = \left(\frac{32}{3}\right)^{1/2} \frac{K_{IC}}{4\Psi\sigma_d d^{1/2}} - \frac{1}{4\Psi} \quad (10)$$

If lateral stresses are modifying the deformation stress then a plot of a/d versus $1/\sigma_d d^{1/2}$ for different particle size fractions, d, will be linear. The value of the radial to axial stress ratio, Ψ and K_{IC} can be determined from the slope and intercept, respectively.

Finally Equation 8 can be rearranged to give a more usable function to allow prediction of the deformation stress to be determined

$$\sigma_d = \left(\frac{32}{3}\right)^{1/2} \frac{K_{IC}}{d^{1/2}} \left(1 - \frac{4\Psi a}{d}\right)^{-1} \quad (11)$$

3. Experimental procedure

3.1. Materials

Sodium chloride (vacuum-dried containing hexacyanoferrate II, an anti-caking agent) was obtained from Chemicals and Polymers Ltd, ICI Runcorn. A range of sizes down to 32 μm was used and the material was sieved using a sieve shaker. Additionally small fractions between 105 and 20 μm were obtained by grinding the 355 μm fraction using a mortar and pestle. Various fractions of the ground material were obtained by sieving using the sieve shaker and an air jet sieve. Median particle size data were calculated form the sieve fraction data.

3.2. Compaction data

Compression was carried out as described previously, the various particle size ranges were compacted using the compression simulator [1]. The deformation stress, σ_d, was determined at a speed of 0.033 mm s^{-1}, as described previously [1] using the following modified Heckel equation

$$\ln\left(\frac{1}{1-D}\right) = \frac{P}{\sigma_d} + B \quad (12)$$

where σ_d is the deformation stress of the particles, whether it is a plastic deformation stress or a fracture deformation stress, or a combination of the two. Data for sodium chloride was adapted from [1] and reproduced in tabular format (Table I) to allow reanalysis of the data.

Tablets were prepared using 590 mg of material for the particle sizes, 64, 116, 196, 328 and 725 μm, respectively, using the compression simulator to allow the fractographic analysis to be performed. A compression pressure of 100 MPa was used because this would allow both fracture and flow to occur within the powder bed (e.g. higher than the yield and fracture stress for sodium chloride).

3.3. Fractographic analysis

Tablets were gold sputter-coated using the coater (Emscope) and the tablet surfaces examined using scanning electron microscopy (Hitachi S2300). For each particle size, crack lengths, a and actual particle diameters, d were determined (Fig. 3 shows an example for a particle size of 725 μm) from a number of photomicrographs for each size. This data was examined below in qualitative analysis.

TABLE I Deformation stresses for the various fractions of sodium chloride, at a punch velocity of 0.033 mm s^{-1}

Material	Median size (μm)	σ_d (MPa)	D_0	D_A
Fraction A	26	89.0	0.550	0.553
Fraction B	36	87.5	0.553	0.566
Fraction C	49	80.8	0.559	0.556
Fraction D	64	76.8	0.549	0.576
Fraction E	83	72.8	0.552	0.566
Fraction F	116	70.5	0.617	0.622
Fraction G	138	70.7	0.627	0.629
Fraction H	196	66.8	0.631	0.626
Fraction I	328	64.7	0.620	0.634
Fraction J	725	64.5	0.589	0.617

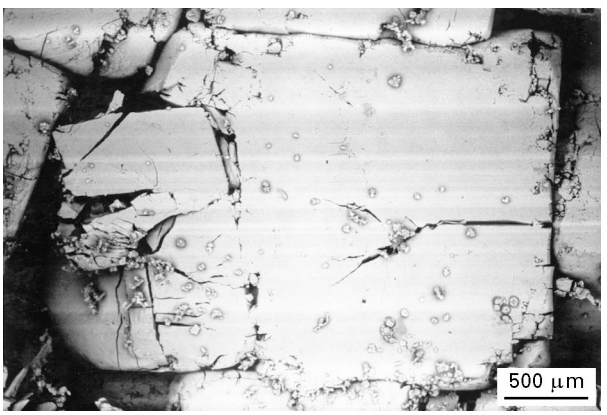

Figure 3 SEM photomicrograph of compacted sodium chloride crystals of 725 μm diameter.

4. Results and discussion

Data from the fractographic analysis is presented in Fig. 4, as a plot of crack length versus particle diameter. A two-term polynomial gave the best fit to the data, with a correlation coefficient of 0.9044 and a standard error of 20.06. The equation of the line is as given in Equation 13

$$a = -7.789858 + 0.240835d + 0.000369d^2 \quad (13)$$

The line intercepts the particle diameter axis at 30.9 μm, very close to the critical particle size, d_{crit}, of 33 μm determined experimentally [1].

In Equation 4 above it was noted that the ratio of the wedge size to the particle size, $w/d = 1/2$. It is interesting to note that in Fig. 3 this was observed in one of the photomicrographs with the crack length extending about half the diameter. Furthermore there seems to be some crack branching as a result of lateral forces.

It is interesting to speculate whether changes in the ratio of the wedge size to the particle size, w/d would affect the cracking or plastic deformation processes within the compact. Equation 4 can be used to examine these effects from a theoretical aspect by determining the effect of w/d on both particle size and the test geometry factor, $A = (32/3)^{1/2}$, using values of $K_{IC} = 0.18$ MPa $m^{1/2}$ and $\sigma_y = 90$ MPa [1] as constants (Fig. 5). Both lines represent the points where the processes change from yielding to fracture (splitting), therefore when $w/d = 1/2$ for large particle sizes and particle sizes below the brittle/ductile transition, splitting and yielding of particles occur respectively. The processes at low and high w/d values are illustrated in Fig. 2 where, in both cases, plastic yielding will occur for a large range of particle sizes.

Fractographic evidence for the occurrence of these other deformation modes was examined in a number of photomicrographs. At low w/d ratios and larger

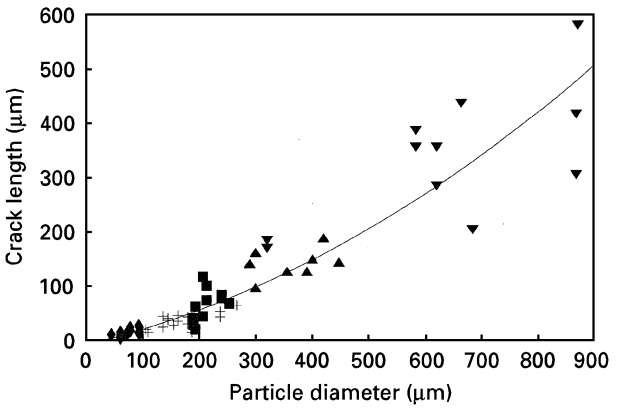

Figure 4 Crack length, a, versus particle diameter, d, for compacted sodium chloride crystals (examination of tablet surfaces): (◆) 64 μm; (+) 116 μm; (■) 196 μm; (▲) 328 μm; (▼) 725 μm.

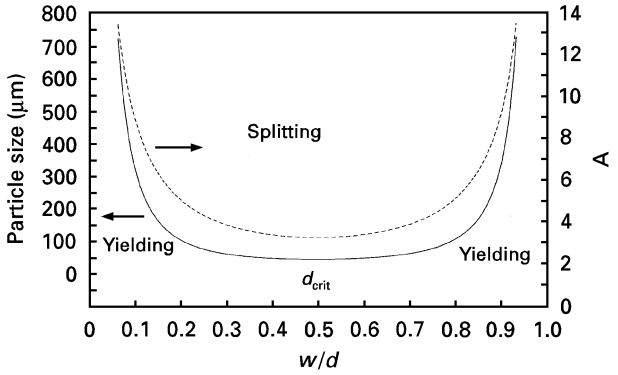

Figure 5 Particle size and A versus w/d for sodium chloride.

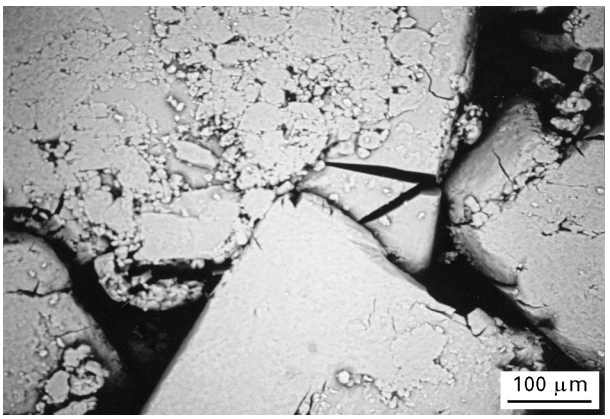

Figure 6 SEM photomicrograph of a sodium chloride crystal of size 180 μm illustrating that the corner of a crystal can act as an indenter.

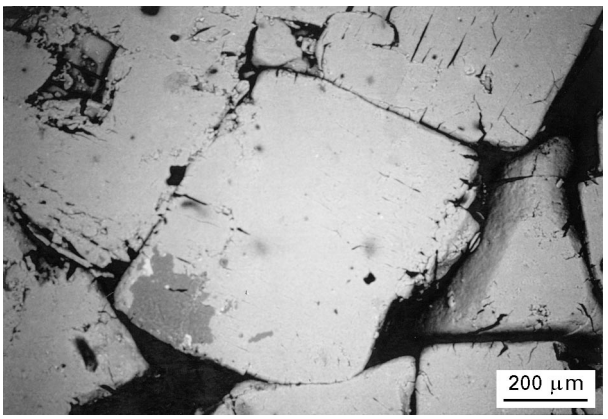

Figure 7 SEM photomicrograph of a sodium chloride crystal of size 328 μm acting as a blunt indenter.

particle sizes (Fig. 5), where a corner of one crystal would act as an indenter into the primary particle (see Fig. 2) deformation would be plastic flow. Evidence for this type of deformation is shown in Fig. 6, although the indenter is also acting as a wedge in this case causing fracture. It is also interesting to note that corner blunting can also occur (Fig. 7) indicative of a size dependency of indenter size (corner of a sodium chloride crystal) on plastic flow. At higher values of w/d ratios and particle sizes (Fig. 5) particle squashing or barrelling (as in Fig. 2) occurs with fragmentation as is evident from Fig. 8.

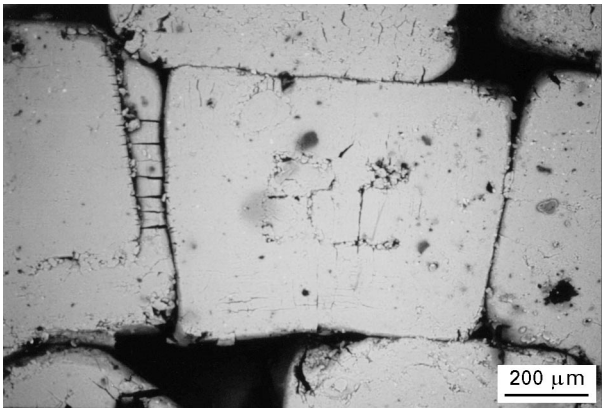

Figure 8 SEM photomicrograph of a sodium chloride crystal of size 328 μm illustrating squashing or barrelling.

It is important to analyse the effect that changes in deformation mode (which is evident from the photomicrographs) on modelling the influence of lateral stresses during compaction. Both the contact zone and the ratio w/d might not be constant (e.g. may not be 0.5 as in Kendall's original derivation (see Fig. 1)). Therefore, the geometry of the cracking process which is essentially modelled on single particle breakage using a specific test geometry factor, α, might not be constant and therefore Equations 8, 10 and 11 will not be predictive.

In Fig. 5 it can be seen that the value of α at the mid point e.g. $w/d = 0.5$ is equivalent to $(32/3)^{1/2}$ or 3.2660 corresponding to Kendall's original derivation, as represented by Equation 9. At the critical particle size for sodium chloride the brittle/ductile upper and lower transitions modes for fracture and flow are the same (i.e. corresponding to the brittle/ductile transition, giving a predicted d_{crit} of 42.7 μm; the same value as in the previous paper [1]). Therefore if the particle size is below this point the platten width has no effect on the mechanism because the particle will always deform plastically. The line in Fig. 5 represents the transition from fragmentation to flow as the contact between deforming particles is changed (e.g. below the line yielding occurs whereas above the line cracking will occur). Over a wide range of w/d values, from approximately 0.3 to 0.7, the value of α does not vary significantly (e.g. from a maximum of 3.8881 at $w/d = 0.3$ and 0.7 to a minimum of 3.2660 at $w/d = 0.5$). Therefore during deformation within the powder bed w/d must be on average 0.5, and other types of deformation must be minimal and consequently $\alpha = (32/3)$, or equivalent to $(32/3)^{1/2}$ in Equation 9.

In Fig. 9 a plot of a/d versus $1/\sigma_d d^{1/2}$ which gives an intercept $1/4\Psi$ and a slope of $(32/3)^{1/2}\ K_{IC}/4\Psi$, as in Equation 10. From this a value of $K_{IC} = 0.1507$ MPa m$^{1/2}$, and a value of radial to axial stress, Ψ, of 0.36 is found from the slope and intercept, respectively. This compares with a value of $K_{IC} = 0.18$ MPa m$^{1/2}$ [1] and indicates that the theory seems to fit the data well. Additionally when $\sigma_d = \sigma_y$, i.e. when no cracks are present in the particles or $a/d = 0$, then the particle size, d_{crit} can be determined from the intercept on the x-axis, $1/\sigma_y d^{1/2}$, (e.g. when $d = d_{crit}$). Using a value of

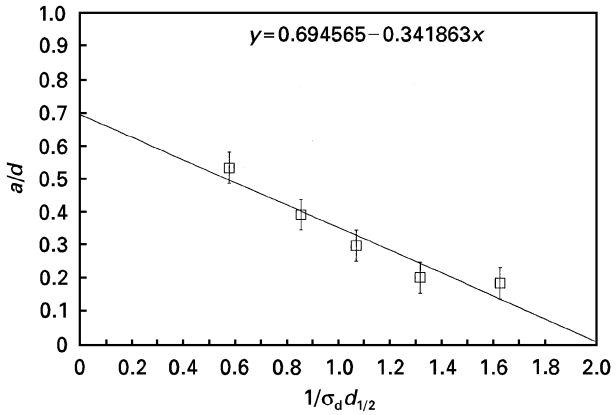

Figure 9 Plot of a/d versus $1/\sigma_d\, d^{1/2}$ for sodium chloride crystals during compaction.

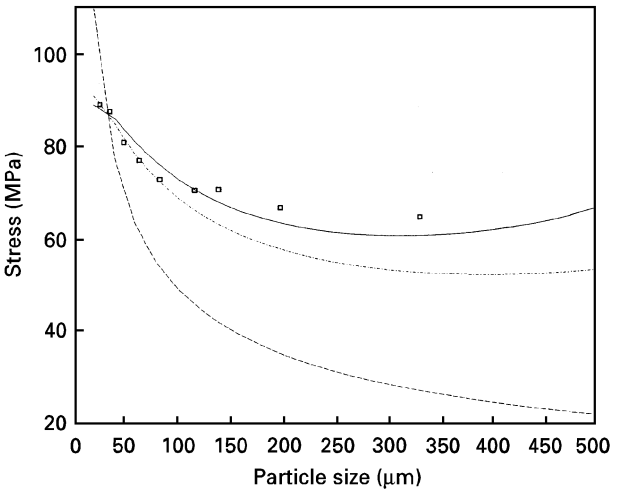

Figure 10 Stress versus particle diameter: (□) experimental data; (·····) $\Psi = 0.36$ (Equation 11); (——) $\Psi = 0.41$ (Equation 11); (- - -) fracture stress curve (Equation 9) using $K_{IC} = 0.15\ \text{MPa m}^{1/2}$ as the constant in both Equations 11 and 9.

$\sigma_y = 90$ MPa [1] the value of d_{crit} determined from the intercept is 29.9 μm; again in good agreement with the experimental data [1]. In addition, the value of the radial to axial stress, Ψ, agrees with that as used by Duncan-Hewitt and Weatherly [6] in their modelling of uniaxial compaction for plastic materials (value of 0.4).

It is interesting to note the similarities in the Duncan-Hewitt and Weatherly approach [6] to that used here. They essentially used both Vicker's hardness data (the stress term) and contact area (to determine the porosity term) to predict the densification for sodium chloride and potassium chloride samples according to Heckel plots [6], whereas in this approach only the stresses are modelled.

Finally an additional proof of the applicability of the model to the die compaction of sodium chloride can be determined by using values of $K_{IC} = 0.15\ \text{MPa m}^{1/2}$, $\Psi = 0.36$ and the algorithm for crack length, a, (Equation 13) in Equation 11 for a range of particle sizes (d). This is shown in Fig. 10, together with the fracture stress line (no lateral forces applied) generated using $K_{IC} = 0.15\ \text{MPa m}^{1/2}$ as the constant in Equation 9. As would be expected the fracture stress line is much lower than the experimental data, and the predicted data using the model. The predicted data using $\Psi = 0.36$ gives good agreement for particles sizes below 100 μm but a poorer fit between 116–328 μm. However with a value of $\Psi = 0.41$, a better fit to the experimental data over a wider range of particle sizes is obtained (20–350 μm). It should be noted however that at 725 μm the predicted deformation stress for $\Psi = 0.41$ is 35 MPa greater than experiment, however when $\Psi = 0.36$ the predicted value is 64.1 MPa which is in good agreement with experiment (Table I).

This difference may arise because the crack length at large particle sizes is a different function of the particle diameter. A value of $a = 316.4$ μm was determined from Equation 11 using values of $d = 725$ μm, $K_{IC} = 0.15\ \text{MPa m}^{1/2}$, and $\Psi = 0.41$; this is much lower than that used in Equation 13, thus supporting this hypothesis. Additionally the largest particle size shows the greatest variability in crack sizes (Fig. 4) (e.g. mean crack length = 370.7 μm with a standard deviation of 106.8 μm). The fact that the variability is greater at larger particle sizes might be because of additional wall effects which have not been taken into account, as the particle size represents 7% of the total die diameter (10 mm). Despite this anomaly, the applicability of the model over a range of particle sizes typically encountered during compaction of pharmaceutical powders (which tend to be < 200 μm) is very good. However, for the model to be applied universally, the relationship between crack length and particle size needs to be determined for a wider number of materials.

References

1. R. J. ROBERTS, R. C. ROWE and K. KENDALL, *Chem. Engng Sci.* **44** (1989) 1647.
2. R. W. HECKEL, *Trans. Metall. Soc. AIME*, **221** (1961a) 671.
3. *Idem., ibid.* **221** (1961b) 1001.
4. K. KENDALL, *Proc. R. Soc. Lond.* **A361** (1978) 245.
5. *Idem., Nature* **272** (1978) 272.
6. W. C. DUNCAN-HEWITT and G. C. WEATHERLY, *J. Pharm. Sci.* **79** (1990) 147.

Received 11 July 1996
and accepted 3 February 1997